**Short Communication**

# Monovalent currents through the T-type $Ca_V3.1$ channels and their block by $Mg^{2+}$

M. Kurejová, M. Pavlovičová and Ľ. Lacinová

*Institute of Molecular Physiology and Genetics, Centre of Excellence for Cardiovascular Research, Slovak Academy of Sciences, Slovakia*

**Abstract.** We have investigated the permeability of the $Ca_V3.1$ channel for $Ca^{2+}$ and different monovalent cations and the block of the currents by $Mg^{2+}$ ions. In the absence of extracellular divalent cations, the $Ca_V3.1$ channel was more permeable for $Na^+$ than for $Cs^+$ and impermeable for $NMDG^+$. Monovalent currents were inhibited by $Mg^{2+}$ of near physiological concentration by three orders of magnitude more effectively than the $Ca^{2+}$ current. Inhibition of outward, but not inward current by $Mg^{2+}$ was voltage-dependent. Furthermore, magnesium slowed down channel deactivation presumably by interacting with an open channel state.

**Key words:** T-type calcium channel — $Ca_V3.1$ — Monovalent cations — Permeability

Family of voltage-activated calcium channels has ten known representatives (for review, see Lacinová 2005). According to their activation potential they are divided into high voltage-activated (HVA) and low voltage-activated (LVA) channels. High selectivity of HVA channels for $Ca^{2+}$ ions is at least partly accomplished by four glutamate residues located in the pore region of the $\alpha_1$ subunit. In contrast to HVA channels, pore region of LVA or the T-type calcium channels contains two glutamates and two aspartates (for review, see Lacinová et al. 2000a). This difference influences not only gating kinetics but also ion selectivity and permeability of the channel (Talavera et al. 2001). Monovalent currents through the cardiac $Ca_V3.2$ T-type calcium channels were analysed by Kaku and coworkers (Kaku et al. 2003). In our work, we concentrated on the analysis of the permeability of neuronal $Ca_V3.1$ channel and its sensitivity towards extracellular $Mg^{2+}$ ions.

We have analysed divalent and monovalent currents through the $Ca_V3.1$ channel permanently expressed in HEK 293 cell line (Lacinova et al. 2002). Cells were grown as described elsewhere (Kurejova and Lacinova 2006). External solutions used in experiments are summarised in Table 1. Internal solution contained (in mmol/l): 130 CsCl, 5 $MgCl_2$, 5 NaATP, 10 TEACl, 10 EGTA and 10 HEPES. pH of all solutions was adjusted to 7.4 with a hydroxide of a major permeable cation or with HCl in the case of $NMDG^+$-based solution. Whole cell currents were measured using an EPC 10 patch clamp amplifier (HEKA Electronic, Lambrecht, Germany). The holding potential in all experiments was –100 mV. Patch pipettes were pulled from borosilicate glass. When filled with pipette solution, their input resistance ranged between 1.8 and 2.0 MΩ. Typical cell capacitance was between 10 and 30 pF. Access resistance was typically between 3.0 and 5.0 MΩ and was compensated up to 70%. Data were recorded with HEKA Pulse 8.30 software package and analysed off-line with HEKA Pulsefit 8.30 software and with Origin 7.5 software (OriginLab Co., Northampton, MA, USA). All values are given as mean ± S.E.M.

$Ca_V3.1$ channels were expressed in HEK 293 cell line with high efficiency, as documented by high density of the current carried by 2 mmol/l $Ca^{2+}$ (Figure 1A and Table 2). In the absence of divalent cations, monovalent cation may permeate through voltage-gated calcium channels (Fukushima and Hagiwara 1985; Lux et al. 1990; Carbone et al. 1997; Kaku et al. 2003). Indeed, when both $Ca^{2+}$ and $Mg^{2+}$ ions were absent from extracellular solution, substantial inward current was carried by $Na^+$ and/or $Cs^+$ ions (Figure 1B,C and Table 2). Organic monovalent cations $NMDG^+$ were not permeable through the $Ca_V3.1$ channel in inward direction. The only channels endogenously expressed in

Correspondence to: Ľubica Lacinová, Institute of Molecular Physiology and Genetics, Centre of Excellence for Cardiovascular Research, Slovak Academy of Sciences, Vlárska 5, 833 04 Bratislava, Slovakia
E-mail: lubica.lacinova@savba.sk

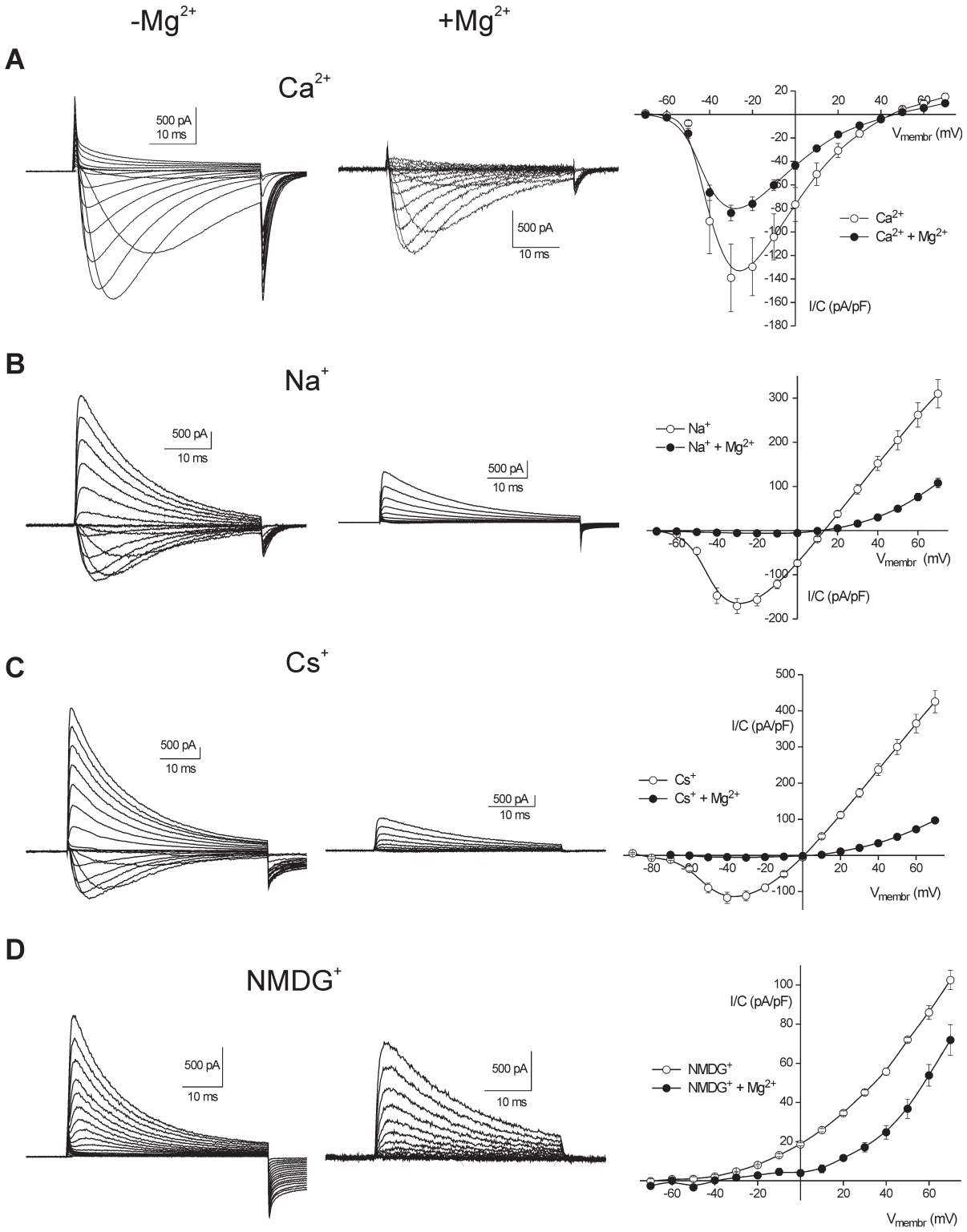


**Figure 1.** Divalent and monovalent currents through the $Ca_v3.1$ T-type channels. Examples of current traces measured in the absence (left column) or in the presence (middle column) of 1 mmol/l $Mg^{2+}$ and averaged current-voltage relations (I-V, right column) for the current amplitudes measured in the absence (○) or in the presence (●) of $Mg^{2+}$. Data are presented for $Ca^{2+}$ solution (A), for $Na^+$ solution (B), for $Cs^+$ solution (C) and for $NMDG^+$ solution (D). Currents were activated by series of depolarizing pulses from a holding potential of –100 mV to membrane voltages marked on axis x of each respective I-V. Solid lines are simple connectors of experimental data.

**Table 1.** Composition of external solutions used in experiments. All concentrations are in mmol/l. For simplicity, individual solutions were given short names, which are used throughout the article

| Short name | NMDG | $CaCl_2$ | $MgCl_2$ | NaCl | CsCl | EGTA | HEPES |
|---|---|---|---|---|---|---|---|
| $Ca^{2+}$ | 160 | 2 | –/1 | – | – | – | 10 |
| $Na^+$ | 70 | – | –/1 | 70 | – | 4 | 10 |
| $Cs^+$ | – | – | –/1 | – | 140 | 4 | 10 |
| $NMDG^+$ | 160 | – | –/1 | – | – | 4 | 10 |

**Table 2.** Properties of individual currents through the $Ca_v3.1$ channel

| External cation (*n*) | $I_{max}$ (pA/pF) | $V_R$ (mV) |
|---|---|---|
| $Ca^{2+}$ (15) | -140 ± 29 | +46.4 ± 1.5 |
| $Ca^{2+}$ + $Mg^{2+}$ (25) | -85 ± 7 | +46.0 ± 1.2 |
| $Na^+$ (22) | -174 ± 17 | +13.7 ± 0.8 |
| $Na^+$ + $Mg^{2+}$ (8) | -7 ± 1 | +10.2 ± 0.7 |
| $Cs^+$ (11) | -118 ± 15 | +0.7 ± 0.9 |
| $Cs^+$ + $Mg^{2+}$ (16) | -9 ± 1 | +5.2 ± 1.3 |
| $NMDG^+$ (6) | +103 ± 5 | – |
| $NMDG^+$ + $Mg^{2+}$ (7) | +72 ± 8 | – |

*n*, the number of cells investigated with each external cation; $I_{max}$, average current density of the inward current measured at a peak of each I-V relation except for current measured in the NMDG solution (in this case, the averaged outward current amplitude measured during depolarizing pulse to +70 mV is given); $V_R$, reversal potential evaluated by interpolation between current amplitudes measured during depolarizing pulses activating the last inward and the first outward current.

HEK 293 cells, which are able to carry high-density outward current, are potassium channels and chloride channels, i.e., channels impermeable for $Cs^+$ ions (Kurejová et al. 2007). Significant outward current was observed in nontransfected HEK 293 cells when potassium was used as major intracellular cation (Kurejová et al. 2007). Nevertheless, nontrasfected HEK 203 cells did not carry outward current, which would have comparable either amplitude or the waveform to that shown in Figure 1B,C,D, when $Cs^+$ was used as a major intracellular cation (Tarabová et al. 2006). Therefore we concluded that positive current observed in all extracellular solutions (Table 1) was $Cs^+$-carried outward current through the expressed $Ca_v3.1$ channels (Figure 1 and Table 2).

In order to evaluate channel selectivity we estimated reversal potential $V_R$ for each type of inward current shown in Figure 1; the results are listed in Table 2. We next calculated selective permeability for $Na^+$ and $Ca^{2+}$ over $Cs^+$ using the modified Goldmann–Hodgkin–Katz equation (Frazier et al. 2000)

$$\frac{P_A}{P_B} = \frac{-z_B^{\,2}([Cs^+]_i - [Cs^+]_o e^{-\nu})(1-e^{-\nu_A})}{z_A^{\,2}([A]_i - [A]_o e^{-\nu_A})(1-e^{-\nu})} \quad (1)$$

where $\nu = V_R$ F/RT and $\nu_A = z_A \nu$. Symbol A refers either to $Na^+$ or to $Ca^{2+}$ ions and $z_A$ refers to their respective charge. For a room temperature of approximately 20°C, at which our experiments were done, calculated and rounded value of F/RT was 0.04. The calculated values of permeability ratios from data in Table 2 using Eq. (1) were $P_{Ca}/P_{Cs}$ = 763 and $P_{Na}/P_{Cs}$ = 3.7 in the absence of $Mg^{2+}$ ions in extracellular solution. Presence of 1 mmol/l of $Mg^{2+}$ shifted reversal potential $V_R$ of $Na^+$-mediated current by 3.5 mV in hyperpolarizing direction (Table 2). This shift caused change in calculated permeability ratio $P_{Na}/P_{Cs}$ = 3.1. Presence of $Mg^{2+}$ had virtually no effect on the reversal potential of $Ca^{2+}$-mediated current (Table 2).

Selectivity of the $Ca_v3.1$ channel for $Ca^{2+}$ over $Cs^+$ ions was more than five-fold lower than selectivity for $Ca^{2+}$ over $Cs^+$ reported for L-type calcium channels (Hess and Tsien 1984; Tsien et al. 1988). The selectivity of T-type calcium channels for $Na^+$ over $Cs^+$ ions has not yet been investigated. Nevertheless, permeability ratio of $Ca_v3.1$ channel $P_{Ca}/P_{Na}$ was found to be 193 (Serrano et al. 2000), i.e., about four-fold lower than permeability ratio $P_{Ca}/P_{Cs}$ found in our work. This finding is in a good agreement with four-fold selectivity of the $Ca_v3.1$ channel for $Na^+$ over $Cs^+$ ions reported here.

Type of the charge carrier may affect kinetics of current activation and inactivation and its voltage-dependence. In order to characterize the voltage-dependence of current activation and inactivation, we have fitted current traces obtained in experiments shown in Figure 1 by the Hodgkin-Huxley equation (Eq. (2))

$$I(t) = I(0)(1-e^{\frac{-t}{\tau_m}})^2(h_\infty + (1-h_\infty)e^{\frac{-t}{\tau_h}}) \quad (2)$$

where I(t) represents current amplitude in the time t, I(0) is maximal current amplitude, $\tau_m$ and $\tau_h$ are time constant of current activation and inactivation, respectively, and $h_\infty$ represents non-inactivating current amplitude. The calculated time constants are plotted as a function of voltage for activation and inactivation in Figure 2A and 2B, respectively.

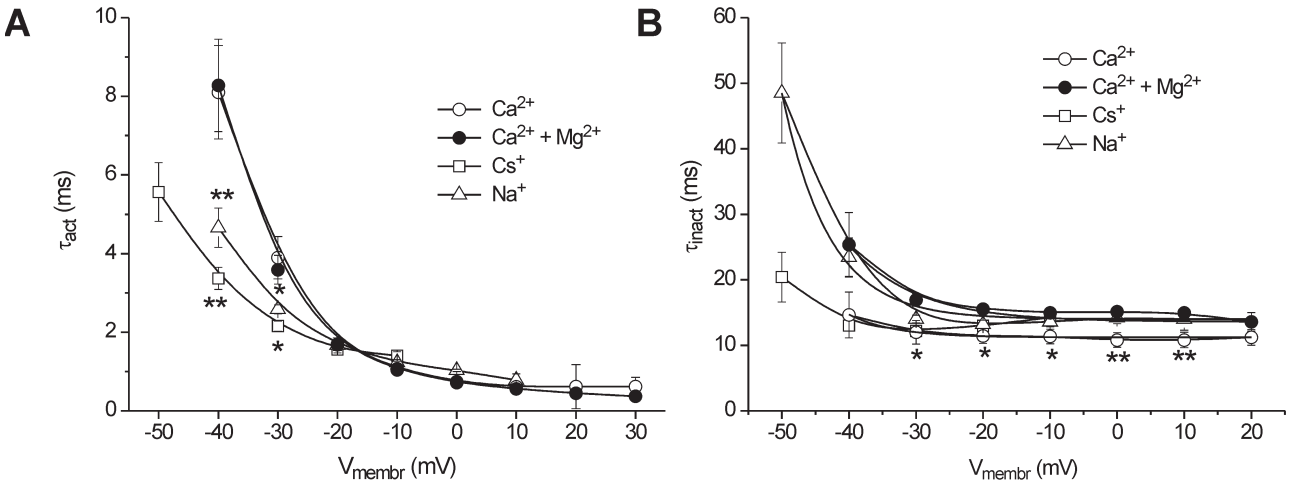


**Figure 2.** Voltage dependence of the activation and inactivation time constants. Time constants of current activation (A) and inactivation (B) were evaluated from current traces measured during I-V protocol (see Figure 1) by fitting individual current traces using the $m^2h$ form of the Hodgkin–Huxley equation. Following charge carriers were investigated: $Ca^{2+}$ (○), $Ca^{2+} + Mg^{2+}$ (●), $Na^+$ (△), $Cs^+$ (□). Significance of the difference between time constants evaluated for $Na^+$, $Cs^+$ or $Mg^{2+}$-inhibited $Ca^{2+}$ current and those for $Ca^{2+}$ current was estimated by unpaired Students *t*-test. * $p < 0.05$; ** $p < 0.01$.

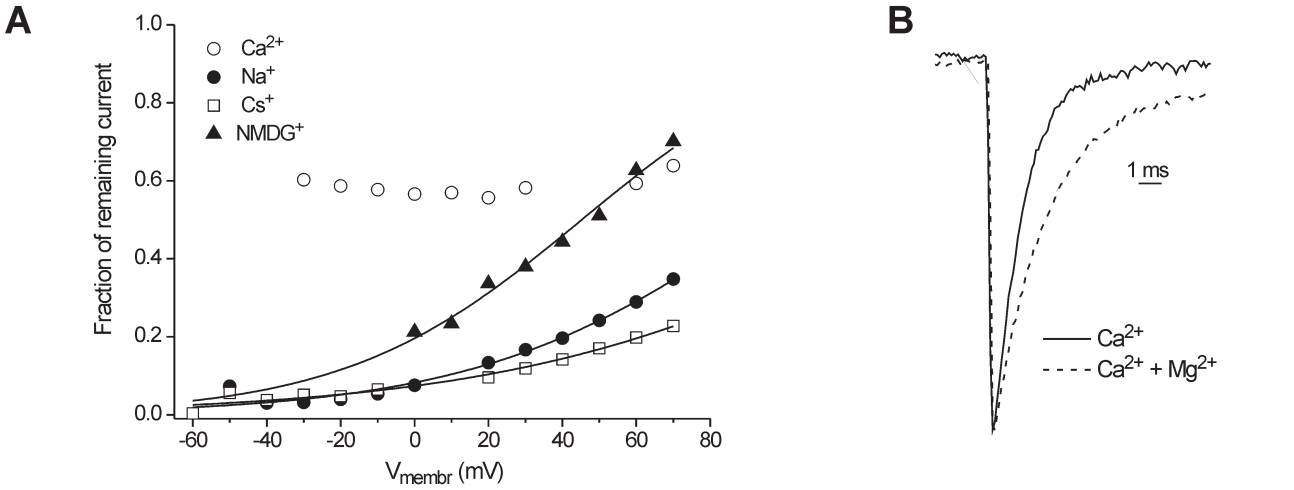


**Figure 3.** Effects of $Mg^{2+}$ on the current through the expressed $Ca_v3.1$ channel. **A.** Relative amplitudes of current remaining in the presence of 1 mmol/l $Mg^{2+}$ were evaluated from I-V relations presented in Figure 1 and are drawn *versus* depolarizing pulse amplitudes. Following solutions were investigated: $Ca^{2+}$ (○), $Na^+$ (●), $Cs^+$ (□), and $NMDG^+$ (▲). Points close to respective reversal potential for each investigated charge carrier were omitted. Solid lines represent fits of experimental data by the Eq. (3). **B.** Examples of tail currents measured during repolarization from +70 mV to the resting membrane potential of –100 mV measured with $Ca^{2+}$ as a charge carrier in the absence (solid line) and the presence (dashed line) of 1 mmol/l $Mg^{2+}$.

The $Ca_v3.1$ channel activated significantly faster at voltages just above the activation threshold when charge carriers were monovalent cations. No significant difference was observed in inactivation time constants between divalent and monovalent currents.

Inhibition of calcium and barium current through the $Ca_v3.1$ channel by relatively high concentration of $Mg^{2+}$ ions (6 mmol/l) was previously investigated (Serrano et al. 2000). In the present study, we have tested how near-physiological concentration of $Mg^{2+}$ ions (1 mmol/l) affects monovalent and

divalent currents through the $Ca_v3.1$ channel. Approximately 40% of $Ca^{2+}$ current was inhibited by 1 mmol/l $Mg^{2+}$ (Figure 1A). On the other side, the same concentration of $Mg^{2+}$ ions was capable to inhibit more than 90% of monovalent inward currents (Figure 1B,C and Table 2). Visual inspection of I-V curves shown in Figure 1 indicated that the inhibition was at least partly voltage-dependent. To quantify this phenomenon, the fraction of the non-inhibited current was calculated for each depolarizing pulse and plotted it *versus* the amplitude of depolarizing pulses (Figure 3A). The extent of inhibition was virtually constant at depolarizing voltages bellow the reversal potential $V_R$ and started to decrease sigmoidally at voltages above the apparent $V_R$, which activated $Cs^+$-mediated outward current. Experimental data for monovalent cations, but not for $Ca^{2+}$ (Figure 3A) were reasonably well fitted by a simplified Woodhull model (Woodhull 1973):

$$f = 1/\{1+[Mg^{2+}]/(K_{D,0}e^{\frac{z\delta FV}{RT}})\} \quad (3)$$

where *f* is the fraction of the current remaining unblocked in the presence of $Mg^{2+}$, $K_{D,0}$ is the dissociation constant (in mmol/l) for $Mg^{2+}$ at 0 mV, z = 2 is the charge of $Mg^{2+}$, and fractional electrical distance $\delta$ is the apparent electrical location of the binding site, expressed as a fraction of the electrical field of the membrane measured from the outside. The obtained values of $K_{D,0}$ were 0.09, 0.08 and 0.24 mmol/l in $Na^+$, $Cs^+$ and $NMDG^+$ solutions, respectively. Parameter $\delta$ showed more uniform trend with values of 0.32, 0.23 and 0.39 for $Na^+$, $Cs^+$ and $NMDG^+$ currents, respectively. These values are in a good agreement with the work of Serrano et al. (2000), who reported $\delta$ = 0.25 and 0.30 for $Mg^{2+}$ block of the current carried through the $Ca_v3.1$ channel by $Ca^{2+}$ or by $Ba^{2+}$ ions, respectively. We can conclude that $Mg^{2+}$ acts at a binding site located approximately at 1/3$^{rd}$ of the electrical field of the cell membrane from the outside. The affinity of this binding site observed in our experiments was by 3–4 orders of magnitude higher than that reported by Serrano et al. (2000) for $Mg^{2+}$ block of the current carried by $Ca^{2+}$ ions (19 mmol/l) or by $Ba^{2+}$ ions (2.7 mmol/l). This is in a good agreement with their assumption that $Ca^{2+}$ ions compete with $Mg^{2+}$ for the same binding site. Our results suggest that similar ion-ion competition takes place also for $Ba^{2+}$ ions but is remarkably weaker, if not absent, for permeable monovalent ions. In the absence of any other divalent cation, this binding site may interact exclusively with magnesium. Three-fold lower apparent affinity in the $NMDG^+$ solution compared to $Na^+$ or $Cs^+$ solutions suggests that $Mg^{2+}$ is less effective in blocking $Na^+$-mediated outward than $Cs^+$-mediated inward current. Our suggestion that magnesium blocked more efficiently $Na^+$ inward current than the $Cs^+$ outward current was further supported by the decrease in permeability ratio $P_{Na}/P_{Cs}$ from 3.7 to 3.1 in the presence of $Mg^{2+}$.

Furthermore, 1 mmol/l of $Mg^{2+}$ affected significantly the kinetics of decay of the $Ca^{2+}$ current. Effect of $Mg^{2+}$ on the kinetics of monovalent currents could not be evaluated because of low amplitude of the inhibited current. Time constants of the $Ca^{2+}$ current decay in the absence and presence of 1 mmol/l $Mg^{2+}$ are compared in Figure 2B. In the absence of $Mg^{2+}$ ions, kinetics of calcium current decay was significantly faster when current was activated by depolarising pulses to voltages between –30 mV and +10 mV (Figure 2B). Current decay during depolarising pulse reflects channel transition from an open into closed and/or inactivated state. Apparently, presence of $Mg^{2+}$ ions obstructed such transition. State-dependent interaction of $Mg^{2+}$ ions with the $Ca_v3.1$ channel should affect kinetics of channel deactivation, too. Therefore, we have fitted tail currents measured during repolarization from +70 mV to –100 mV, i.e., tail currents of the last trace measured during an I-V protocol (Figure 3B) by a single exponential function. Presence of 1 mmol/l of $Mg^{2+}$ increased the time constant of current deactivation from 2.19 ± 0.23 ms ($n$ = 13) to 3.13 ± 0.15 ms ($n$ = 18). These values were significantly different ($p < 0.01$, unpaired Student's t-test). This observation is in contrast with previously published findings that $Ni^{2+}$ and $Cd^{2+}$, other divalent cations accelerate calcium channel deactivation during channel block (Lacinova et al. 2000b). Slowing down the deactivation time constant by $Mg^{2+}$ suggests that: i) deceleration of current decay may reflect obstructed transition of channel into closed state, too; and ii) $Mg^{2+}$ must first unbind from its binding site before the channel can close. $Ni^{2+}$ and $Cd^{2+}$ ions interact with the $Ca_v3.1$ channel by a different mechanism, which remains to be determined.

Inhibition of monovalent currents through the T-type calcium channel by $Mg^{2+}$ was described previously in chick sensory neurons (Lux et al. 1990; Carbone et al. 1997), where all three $Ca_v3.n$ channels are expressed with dominant expression of $Ca_v3.2$ channel (Heppenstall and Lewin 2006). In these cells, $Mg^{2+}$ blocked $Na^+$ current by three orders of magnitude more potent than the $Ca^{2+}$ current. We have confirmed this observation for a well-defined single population of $Ca_v3.1$ channels and extended it for another monovalent cation, $Cs^+$.

To summarize, we have shown that permeability and partly also gating kinetics of the $Ca_v3.1$ channel depends on the combination of external and internal ions. Physiological concentration of $Mg^{2+}$ ions blocks this channel in its open state by competing for binding site accessible from the outer site of cell membrane. Binding of $Mg^{2+}$ to this site can almost fully prevent entry of monovalent cations, but is relatively ineffective in preventing of the flow of the outward current carried by $Cs^+$ ions.

**Acknowledgments.** We thank S. Mannova for excellent technical assistance. Supported by grants VEGA 2/7001 and APVV-51-027404.

## References


Carbone E., Lux H. D., Carabelli V., Aicardi G., Zucker H. (1997): $Ca^{2+}$ and $Na^+$ permeability of high-threshold $Ca^{2+}$ channels and their voltage-dependent block by $Mg^{2+}$ ions in chick sensory neurones. J. Physiol. **504,** 1–15

Frazier C. J., George E. G., Jones S. W. (2000): Apparent change in ion selectivity caused by changes in intracellular $K^+$ during whole-cell recording. Biophys. J. **78,** 1872–1880

Fukushima Y., Hagiwara S. (1985): Currents carried by monovalent cations through calcium channels in mouse neoplastic B lymphocytes. J. Physiol. **358,** 255–284

Heppenstall P. A., Lewin G. R. (2006): A role for T-type $Ca^{2+}$ channels in mechanosensation. Cell Calcium **40,** 165–174

Hess P., Tsien R. W. (1984): Mechanism of ion permeation through calcium channels. Nature **309,** 453–456

Kaku T., Lee T. S., Arita M., Hadama T., Ono K. (2003): The gating and conductance properties of $Ca_v3.2$ low-voltage-activated T-type calcium channels. Jpn. J. Physiol. **53,** 165–172

Kurejová M., Lacinová Ľ. (2006): Effect of protein tyrosine kinase inhibitors on the current through the $Ca_v3.1$ channel. Arch. Biochem. Biophys. **446,** 20–27

Kurejová M., Uhrík B., Sulová Z., Sedláková B., Križanová O., Lacinová Ľ. (2007): Changes in ultrastructure and endogenous ionic channels activity during culture of HEK 293 cell line. Eur. J. Pharmacol. **567,** 10–18

Lacinova L. (2005): Voltage-dependent calcium channels. Gen. Physiol. Biophys. **24** (Suppl. 1)**,** 1–82

Lacinová Ľ., Klugbauer N., Hofmann F. (2000a): Low voltage activated calcium channels: from genes to function. Gen. Physiol. Biophys. **19,** 121–136

Lacinová Ľ., Klugbauer N., Hofmann F. (2000b): Regulation of the calcium channel $\alpha_{1G}$ subunit by divalent cations and organic blockers. Neuropharmacology **39,** 1254–1266

Lacinová Ľ., Klugbauer N., Hofmann F. (2002): Gating of the expressed $Ca_v3.1$ calcium channel. FEBS Lett. **531,** 235–240

Lux H. D., Carbone E., Zucker H. (1990): $Na^+$ currents through low-voltage-activated $Ca^{2+}$ channels of chick sensory neurones: block by external $Ca^{2+}$ and $Mg^{2+}$. J. Physiol. **430,** 159–188

Serrano J. R., Dashti S. R., Perez-Reyes E., Jones S. W. (2000): $Mg^{2+}$ block unmasks $Ca^{2+}/Ba^{2+}$ selectivity of $\alpha_{1G}$ T-type calcium channels. Biophys. J. **79,** 3052–3062

Talavera K., Staes M., Janssens A., Klugbauer N., Droogmans G., Hofmann F., Nilius B. (2001): Aspartate residues of the Glu-Glu-Asp-Asp (EEDD) pore locus control selectivity and permeation of the T-type $Ca^{2+}$ channel $\alpha_{1G}$. J. Biol. Chem. **276,** 45628–45635

Tarabová B., Kurejová M., Sulová Z., Drabová M., Lacinová Ľ. (2006): Inorganic mercury and methylmercury inhibit the $Ca_v3.1$ channel expressed in human embryonic kidney 293 cells by different mechanisms. J. Pharmacol. Exp. Ther. **317,** 418–427

Tsien R. W., Lipscombe D., Madison D. V., Bley K. R., Fox A. P. (1988): Multiple types of neuronal calcium channels and their selective modulation. Trends Neurosci. **11,** 431–438

Woodhull A. M. (1973): Ionic blockage of sodium channels in nerve. J. Gen. Physiol. **61,** 687–708


Final version accepted: August 28, 2007